



The Utilization of Napier Grass Stems for Cd(II) Ions Removal from Aqueous Solution: Process Optimization Studies Using Response Surface Methodology

Wimonrat Tongpoothorn^{1*}, Titikan Somboon¹ and Manop Sriuttha²

¹Department of Chemistry, Faculty of Engineering, Rajamangala University of Technology Isan, Khon Kaen Campus, Muang, Khon Kaen 40000, Thailand.

²Department of Chemistry, Faculty of Applied Science and Engineering, Khon Kaen University, Nong Khai Campus, Nong Khai 43000, Thailand.

* Corresponding author. E-mail address: wimonrat.to@rmuti.ac.th

Received: 12 February 2019; Revised: 21 February 2020; Accepted: 28 February 2020; Available online: 5 June 2020

Abstract

The aim of this research was to study the utilization of Napier grass stems (NGS) as an adsorbent for removing Cd(II) ions from aqueous solutions. The characteristics of adsorbency indicated that adsorption could occur via electrostatic interaction between metal ions and active functional groups on the rough surfaces of the adsorbent. The conditions of the adsorption process were optimized using the Response Surface Methodology (RSM). The three variables in this study were pH, initial concentration, and adsorbent dosage, which were decided by the Central Composite Design (CCD), while the response was considered by the adsorption capacity. The statistical analysis demonstrated that the proposed model was significant in response, precision, and reliability. The maximum adsorption capacity was 5.90 mg g^{-1} in a solution with a pH of 5.83, an initial concentration of 50.00 mg L^{-1} , and with an adsorbent dosage of 0.10 g . It was found that the initial concentration of Cadmium solution and adsorbent dosage had a significant effect on the adsorption capacity. The equilibrium process of Cadmium adsorption was well-described by the Langmuir adsorption isotherm ($R^2=0.9918$), and the adsorption kinetic corresponded to the pseudo-second order model ($R^2=0.9990$). In addition, thermodynamic studies illustrated that the adsorption process was endothermic and non-spontaneous in nature. In summary, it was proved to be feasible that Napier grass stems could be used as an alternative and sustainable adsorbent for removing Cd(II) ions from aqueous solutions.

Keywords: adsorption isotherm, kinetic study, napier grass stems, optimization, response surface methodology, thermodynamic study

Introduction

Heavy metal ions, such as Pb(II), As(III), Cu(II), Cd(II), Zn(II), and Ni(II), contaminate the waters that are discharged from mining, electronics, various chemical industries, and machinery manufacturing. Such ions are non-biodegradable and cause various diseases or disorders in humans and in aquatic organisms (Bhargavi, Sethuraman, Krishnan, Bosco, & Rayappan, 2015; Li et al., 2011; Sun, Zhou, Xu, Wang, & Liang, 2011). Among these metals, Cd(II) is one of the most dangerous pollutants due to the fact that it can cause cell death, can damage the kidneys, cause bone disease, or can damage lung function (Chabicoovsky, Klepal, & Dallinger, 2004; Xi, Luo, Luo, & Luo, 2015). Accordingly, long-term exposure caused by drinking water containing cadmium, at even trace levels, should be conscientiously disallowed. In order to minimize the unavoidable health risks, the World Health Organization (WHO, 2011) has recommended that the maximum concentration limit of Cadmium be 0.003 mg/L (http://www.who.int/water_sanitation_health/publications/2011/dwq_guidelines/en/). Because of its toxicity, non-degradability, and accumulation, the removal of Cd(II) from water has attracted great attention worldwide (Cai et al.,



2017; Tan et al., 2015). Several techniques, such as chemical precipitation, microbial biotechnology (Wu et al., 2017), pulsed corona plasma discharge (Qu et al., 2013), ion exchange (Wang, Feng, Hao, Huang, & Feng, 2014), electrocoagulation (Al-Shannag, Al-Qodah, Bani-Melhem, Qtaishat, & Alkasrawi, 2015), and membrane processes (Llanos et al., 2010; Zhong et al., 2013) have been reported and employed in removing heavy metals from polluted water. However, limitations in such processes have been found, such as an inefficiency in targeting specific pollutants and the high costs of operations or regeneration. In addition, some processes can generate toxic wastes as byproducts (Al-Malack & Dauda, 2017). Many research studies have reported that adsorption is considered to be one of the most preferred methods for removing heavy metals due to its simple operation, strong controllability, efficiency of high removal, economic considerations, and its sludge-free operations. Additionally, the adsorption process does not generate any secondary pollution by producing harmful substances during the process (Sun et al., 2017; Zhu et al., 2015; Gupta et al., 2015).

Recently, adsorbents, derived from agricultural wastes, industrial by-products, and natural materials, are becoming more attractive due to their bio-degradability, availability, and sustainable advantages (Peng et al., 2016; Leng et al., 2015). It is well known that bio-based adsorbents also contain functional groups, such as carboxylic, hydroxyl, and phenolic groups, which can adsorb metal ions (Guo, Zhang & Shan, 2008). In this research, the utilization of Napier grass stems as adsorbents was investigated due to their low costs (1.6 baht/kg), as well as their ability to grow quickly and to be strongly resistant to water stress. Importantly, such grass is easily accessible as there are large quantities growing in Thailand. Based on the quest for adsorption, both the raw material value for adsorbent production and the cost of the adsorption process were considered. Therefore, efficiently carrying out the experimentation through a process involving the design of experiments (DOE) with the least possible number of experiment runs could lead to the achievement of cost-effective and acceptable results (Dil et al., 2016). DOE is also advantageous for examining the interaction and relationship between variables (Sales, Magriotis, Rossi, Resende, & Nunes, 2013). The selection of the appropriate modeling and optimization approaches is critical for the accuracy of these processes. Response surface methodology (RSM) is an acceptable tool, which has categories, such as central composite design (CCD). In this work, it was used to optimize the adsorption parameters. This tool has simple a structure and provides high efficiency. It further yields a prediction model of response (adsorption capacity) at the optimum operating conditions. The approach provides an advantage for chemical experiments in both preparation and analysis. Also, it provides guidelines for higher reproducibility and repeatability. Its primary merit is that the tool requires a limited number of trials, and thereby, requires less time and costs less (Santra & Sarkar 2016).

In the present work, the applicability and efficiency of using Napier grass stems (NGS) as an alternative natural adsorbent for removing Cd(II) ions from aqueous solutions were investigated. In order to obtain the maximum adsorption capacity, the adsorption conditions were optimized by using RSM with varying parameters of pH solutions, initial cadmium concentrations, and adsorbent dosages. In addition, adsorption kinetics, isotherms, and thermodynamics were studied to evaluate the performance of cadmium removal.



Materials and Methods

Material and reagents

The Napier grass stems were obtained from the Bureau of Animal Nutrition Development in Khon Kaen, Thailand. The stock cadmium standard solution (1000 mg L^{-1}) for AAS was purchased from Merck (Germany). The sodium hydroxide and hydrochloric acid were of analytical grade and were obtained from Carlo Erba (France). The experimental solutions were prepared by properly diluting the stock with deionized water.

Preparation and characterization of adsorbent

The adsorbent was prepared and characterized in accordance with our previous work. Briefly, NGS powder was pre-treated by soaking in 1.0 M sodium hydroxide solution and was then autoclaved at 121°C and at 15 psi for 15 min. After that, it was filtered and washed with distilled water until a neutral pH was obtained. Then, the residual was dried at 80°C to obtain the adsorbent, which was then defined as pre-treated NGS (pNGS). The characteristics of adsorbent were determined by using an FT-IR spectrometer (Spectrum One, PerkinElmer, USA), which recorded in the range of $4000\text{--}450 \text{ cm}^{-1}$ and at a resolution of 4 cm^{-1} . The morphology of the pNGS was determined using a Scanning Electron Microscope (SEM, Hitachi TM3030, Japan) (Wimonrat, Orranooch, Titikan & Manop, 2019).

Adsorption experiments

Batch experiments, which were based on RSM, were carried out by mixing certain amounts of pNGS with 25.00 mL of Cadmium solution in a 250.00 mL bottle, which was then immersed in water bath at 318 K. The range of each parameter is shown in Table 1. After adsorption, the solution and the adsorbent were separated by centrifugation and the remaining Cadmium concentration in the solution was determined by using a Flame Atomic Absorption Spectrophotometer (FAAS, AA-240FS, Varian, USA) at a wavelength of 228 nm. The adsorption capacity (q_e , mg g^{-1}) was calculated by solving the following equation (1):

$$q_e = \frac{(C_0 - C_e) V}{W} \quad (1)$$

in which... q_e was the adsorption capacity (mg g^{-1}), C_0 and C_e were the initial and equilibrium concentrations of the cadmium solutions (mg L^{-1}), respectively. V was the volume of the batch solution (L), and W was the adsorbent dosage (g) used in the experiments (Denizli, Özkan, & Arica, 2000).

Optimized condition using RSM

For the purpose of obtaining the maximum adsorption capacity, the experiments for the optimized condition were performed by using RSM with CCD. The three analytical parameters consisting of the pH of the Cadmium solution (A: 4–6), the initial Cadmium concentration (B: 10–50 mg L^{-1}), and the adsorbent dosage (C: 0.10–0.30 g) were assigned as independent variables. For each set of experiments, the contact time remained fixed at the equilibrium time. The levels and codes of the variables are shown in Table 1. These consisted of 20 experiments, which had been designed by the Design Expert software (version 7.0.0, Stat. Ease. Inc, United States) statistical package. For the optimization process, the response can be simply related to the chosen factors by the second order equation and is given as Eq. (2):



$$Y = \beta_0 + \beta_1 A + \beta_2 B + \beta_3 C + \beta_{12} AB + \beta_{13} AC + \beta_{23} BC + \beta_{11} A^2 + \beta_{22} B^2 + \beta_{33} C^2 \quad (2)$$

in which... Y was the process response (adsorption capacity) and A, B and C represented the effect of the independent variables. Thus, A^2 , B^2 , and C^2 were the square effects and AB, AC, and BC were the interaction effects; β_0 was the regression coefficient at the center point; β_1 , β_2 , and β_3 were the linear coefficients; β_{12} , β_{23} , and β_{13} were the interaction coefficients; and β_{11} , β_{22} , and β_{33} were the quadratic coefficients. The adequacy of the proposed model was then exhibited using the diagnostic checking tests provided by analysis of variance (ANOVA). The optimum values of the parameters were examined by solving the regression equation and by analyzing the surface of the 3D and the contour plots.

Table 1 The levels and codes of variables in CCD statistical experimental design

Independent variables	Symbol	Code variable level		
		Low (-1)	Center (0)	High (+1)
pH of cadmium solution	A	4	5	6
initial cadmium concentration (mg L ⁻¹)	B	10	30	50
adsorbent dosage (g)	C	0.10	0.20	0.30

Adsorption Kinetics

The kinetics studies may be defined as tests necessary for the establishment of the mechanism of adsorption. Different types of kinetic models were available in the literature. Moreover, the majority of them showed that the kinetics of adsorption could be described by models of pseudo-first order (Lagergren, 1898) and pseudo-second order (Ho & Mckay, 1999). These are present in Equations (3) and (4), respectively.

$$\frac{1}{q_e} = \frac{k_1}{q_e} \frac{1}{t} + \frac{1}{q_e} \quad (3)$$

$$\frac{t}{q_t} = \frac{1}{k_2 q_e^2} + \frac{t}{q_e} \quad (4)$$

in which ... q_e and q_t represented the amounts of metal ions, which had been adsorbed at equilibrium and time t , respectively. k_1 was the rate constant of the pseudo-first order equation (min^{-1}), whereas k_2 was the rate constant of the pseudo-second order equation ($\text{g mg}^{-1} \text{min}^{-1}$).

Adsorption isotherms

In general, the adsorption isotherm describes the relationship between the metal ion in liquid phase and metal ion sorbed on adsorbent at a constant temperature (Tatah, Ibrahim, Ezeonu, & Otitoju, 2017). To quantify the adsorption capacity of the sorbent for cadmium adsorption, two models namely Langmuir (1918) and Freundlich (1906) were adopted in this work and are represented by the following linear equation (5) and (6), respectively:

$$\frac{1}{q_e} = \frac{1}{q_m} + \frac{1}{K_L q_m} \frac{1}{C_e} \quad (5)$$



in which ... q_e and q_m were the equilibrium adsorption capacity and the maximum adsorption capacity per gram of dry weight of the adsorbent, respectively. C_e was expressed in mg L^{-1} , and K_L was an equilibrium constant (L mmol^{-1}).

$$\ln q_e = \ln K_F \left(\frac{1}{n} \right) \ln C_e \quad (6)$$

in which ... K_F was a constant (mmol g^{-1}) and $1/n$ was a constant related to the adsorption intensity (Liqiang et al., 2019).

Adsorption thermodynamics

The thermodynamic characterization of the solid-liquid interface is important in the context of understanding the adsorption mechanism (Sales et al., 2013). Therefore, the effects of temperature on the adsorption of Cadmium ions was studied at temperatures of 298 K, 313 K, 328 K, and 343 K. Thermodynamic parameters were calculated by the following equations (7) and (8):

$$\ln \frac{q_e}{C_e} = \frac{\Delta S^\circ}{R} - \frac{\Delta H^\circ}{RT} \quad (7)$$

$$\Delta G^\circ = \Delta H^\circ - T\Delta S^\circ \quad (8)$$

in which ... ΔG° (kJ mol^{-1}) was the Gibbs free energy change, R ($8.314 \text{ J mol}^{-1}\text{K}^{-1}$) was the universal gas constant, T (K) was the temperature, ΔH° (kJ mol^{-1}) was the enthalpy, and ΔS° ($\text{kJ mol}^{-1}\text{K}^{-1}$) was the entropy change (Herbert et al., 2016).

Results and Discussion

The FT-IR spectra of the pNGS is shown in Figure 1. The presence of active functional groups was observed, such as hydroxyl, carbonyl, and carboxyl groups, which are potentially active in binding metals (Pavan, Lima, Dias, & Mazzocato, 2008; Runping et al., 2010). However, rather similar characteristics of both spectra were observed, suggesting that chemical bonds had neither been broken nor created. Therefore, the binding of active site on the surface of pNGS and Cd(II) could be involved with the electrostatic interaction. Moreover, the rough and irregular surface of pNGS in the micrograph had provided favorable conditions for ion-surface interaction.

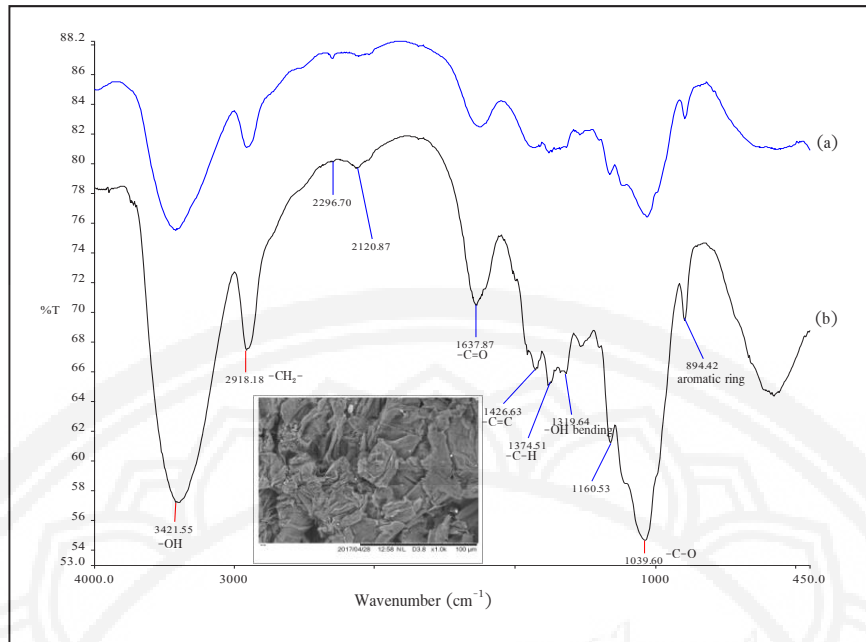


Figure 1 SEM photograph and FT-IR spectra of pNGS before (a) and after (b) Cd(II) adsorption

Optimization of significant variables by CCD

The experimental adsorption capacity was observed in the range of 0.00–6.39 mg g⁻¹ (Table 2).

Table 2 Central composite design matrix for the experimental design and the response

Run	Factor1 A: pH	Factor2 B: Initial Concentration (mg L ⁻¹)	Factor3 C: Adsorbent dosage (g)	Response Adsorption capacity (mg g ⁻¹)
1	6.00	50.00	0.30	3.26
2	4.00	10.00	0.30	0.80
3	5.00	63.40	0.20	4.78
4	5.00	30.00	0.20	2.62
5	4.00	50.00	0.10	5.26
6	3.32	30.00	0.20	1.89
7	5.00	30.00	0.20	2.66
8	4.00	10.00	0.10	1.71
9	6.68	30.00	0.20	2.84
10	5.00	30.00	0.03	6.39
11	5.00	0.00	0.20	0.00
12	5.00	30.00	0.20	0.76
13	6.00	10.00	0.10	2.06
14	5.00	30.00	0.37	1.77
15	6.00	10.00	0.30	0.92
16	5.00	30.00	0.20	2.66
17	5.00	30.00	0.20	2.74



Table 2 (Cont.)

Run	Factor1 A: pH	Factor2 B: Initial Concentration (mg L ⁻¹)	Factor3 C: Adsorbent dosage (g)	Response Adsorption capacity (mg g ⁻¹)
18	4.00	50.00	0.30	3.18
19	5.00	30.00	0.20	2.72
20	6.00	50.00	0.10	5.52

Validity testing of CCD model using ANOVA

Analysis of variance (ANOVA) evaluated (i) the significance of the linear and quadratic effects of the variables on the predicted response and (ii) the quality of the design model as shown in Table 3. The obtained F-value of 43.29 and the p-value (Prob>F) of less than 0.05 implied that model, and the terms of B, C, BC, and C² were found to be significant. The quality of the derived polynomial was examined from the regression coefficient (R²), the adjust R² (R²_{adj}), the predicted R² (R²_{pred}), and the adequate precision (AP). The high R² (0.9750) and R²_{adj} (0.9525), as well as their reasonable agreement, illustrated a high degree of correlation between the calculated and observed results within the range of the experiments. However, the extent of residual may be estimated from R²_{pred} (0.8055) and from AP (23.461) (adequate precision > 4), which represent an adequate signal for the model. The residual was the sum of lack of fit and a pure (random) error. Here, the lack of fit F-value of 82.26 indicated that there may have been some systematic variation, which had been unaccounted for in the hypothesized model. This may have been due to the exact replicate values of the independent variable in the model that had provided the estimate of pure error. The precision was estimated from SD (0.35), C.V. (12.47%), and PRESS (9.66), which were low and which confirmed that the statistical model, obtained from this study, had been both accurate and reliable. A small contribution of pure error (2.987E-003) to SS suggested the validity of the design and the model (Santra & Sarkar, 2016; Montgomery, 2008).

Table 3 ANOVA for response surface reduced quadratic model

Source	Sum of squares	df	Mean square	F value	p-value prob > F
Model	48.44	9	5.38	43.29	< 0.0001
A-pH	0.42	1	0.42	3.41	0.0944
B-Initial conc.	28.89	1	28.89	232.32	< 0.0001
C-Adsorbent dosage	14.68	1	14.68	118.08	< 0.0001
AB	2.113E-003	1	2.113E-003	0.017	0.8989
AC	0.021	1	0.021	0.17	0.6897
BC	0.66	1	0.66	5.27	0.0445
A ²	0.24	1	0.24	1.89	0.1991

**Table 3** (Cont.)

Source	Sum of squares	df	Mean square	F value	p-value prob > F
B ²	0.42	1	0.42	3.34	0.0976
C ²	3.32	1	3.32	26.69	0.0004
Residual	1.24	10	0.12		
Lack of fit	1.23	5	0.25	82.26	<0.0001
Pure error	0015	5	2.987E-003		

$R^2=0.9750$, $R_{adj}^2=0.9525$, $R_{pred}^2=0.8055$, AP= 23.461

Model validation through regression plot

The accuracy and validity of the model were investigated from regression plots viz. plot of actual versus predicted (model) response and normal probability plot of the studentized residuals. A well correlation of actual and predicted response (Figure 2 (a)) indicated the accuracy of the model.

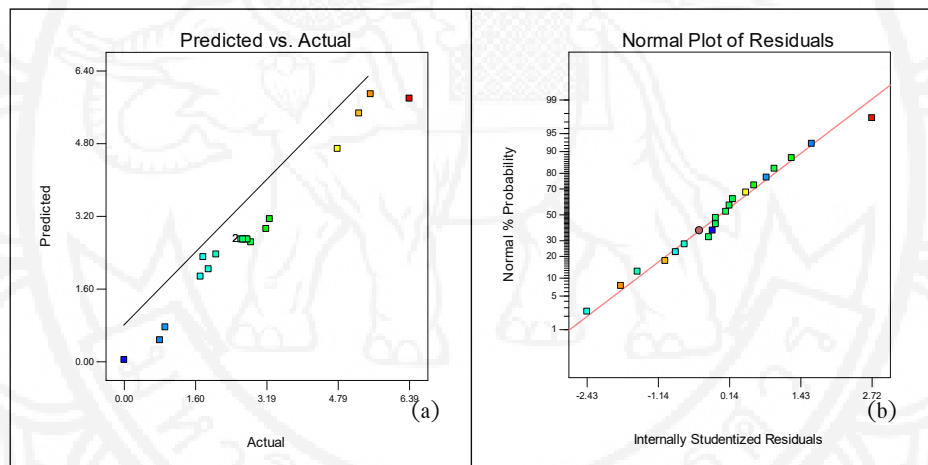


Figure 2 Plot of actual versus predicted response(a) and normal probability plot (b)

A normal probability plot indicates that for a normal distribution of the residuals, the data points should lie on a straight line. In the present case, the small scattering of the data observed (Figure 2 (b)) was determined to be within the limits of random error (Santra & Sarkar, 2016).

The optimized condition and effects of variables on adsorption capacity

In order to understand the effects of each variable, the responses were estimated via contour and three dimension (3D) plots. The base of the model was a polynomial function for analysis. The investigation of the interactive effect of two variables on the adsorption capacity within the experimental ranges is presented in Figure 3. A second order polynomial in terms of actual factors, as well as an empirical relationship between adsorption capacity (Y) and process variables, can be expressed by the quadratic model in terms of code factors as follows:



$$Y = +2.69+0.18*A+1.49*B-1.04*C-0.016*A*B-0.051*A*C- 0.29*B*C- 0.13*A^2-0.18*B^2-0.48*C^2 \quad (9)$$

With the largest coefficient of initial concentration, (B) was determined to be the most effective influenced variable (as Eq.9). The positive sign of this coefficient meant that the adsorption capacity was favorable at high values of initial concentration due to the fact that more adsorbate molecules had been adsorbed onto the surface of the pNGS (Saad et al., 2017). Furthermore, the mass transfer driving force between the aqueous and solid phases had been increased. Another variable affecting the response was the adsorbent dosage (C). Its coefficient showed a negative sign, which indicated that the number of Cd(II) ions was under the limit. At the low adsorbent dosage, the adsorption was quick and became efficiently saturated, while at higher adsorbent dosages, more active adsorption sites were available, which led to a lower adsorption capacity (Karimi et al, 2016) from only the interaction between the initial concentration and the adsorbent dosage (BC), whereas the quadratic effects of adsorbent dosage (C^2) on the adsorption capacity were found to be significant.

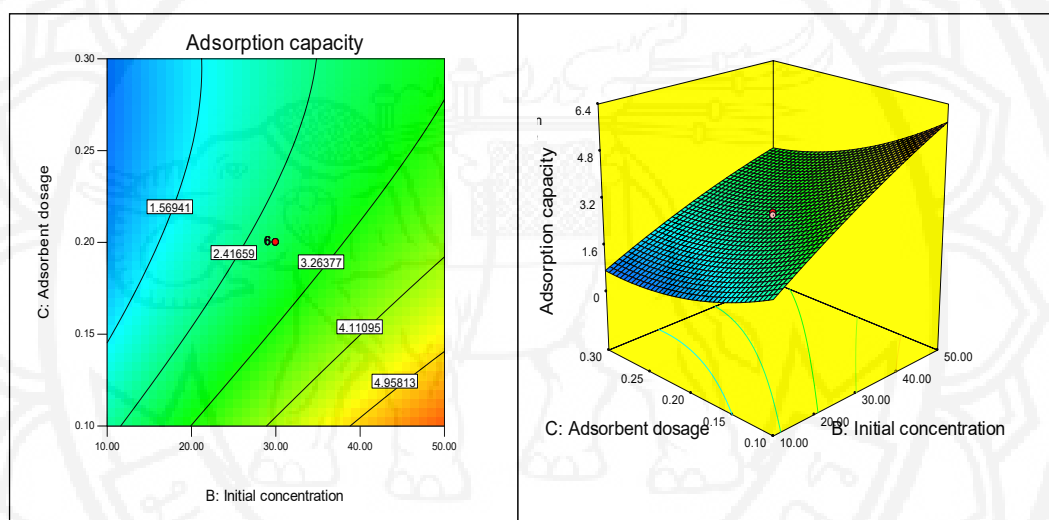


Figure 3 Contour and 3D surface plots of response surfaces for combined effects of significant variables between initial concentration and adsorbent dosage

In Figure 3, the contour and 3D surface plots illustrate that from the initial concentration until 50 mg L^{-1} , the adsorption capacity had increased with the growth, but had decreased with higher amounts of adsorbent dosages. The optimum conditions, which were calculated by the software consisted of a pH value of 5.83, an initial concentration of 50 mg L^{-1} , and an adsorbent dosage of 0.10 g. It showed an adsorption capacity of 5.90 mg g^{-1} with a desirability of 0.922 (Figure 4). Under these conditions, the results from the experiment showed an average adsorption capacity of $5.89 \pm 0.02 \text{ mg g}^{-1}$ (N=3) with a relative standard deviation (%RSD) of 0.36.

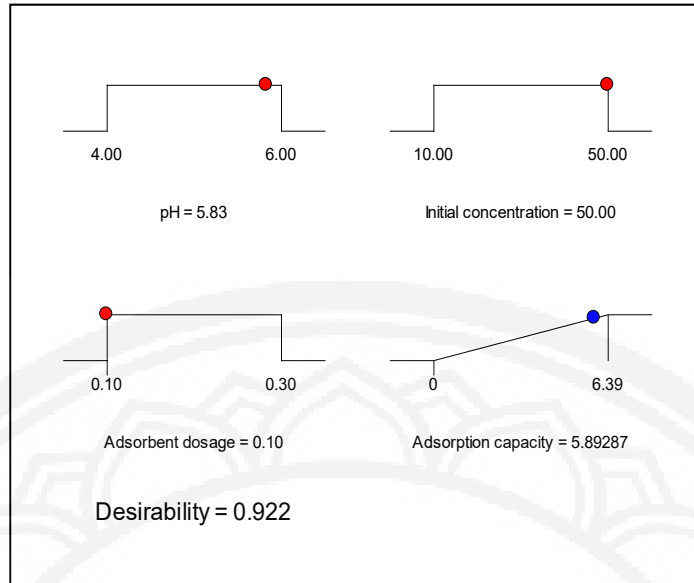


Figure 4 The optimum condition calculated by software

Kinetic study

In order to investigate the adsorption mechanisms of Cadmium ion adsorption on pNGS, the pseudo-first order and pseudo-second order kinetic models were investigated. The results are shown in Figure 5 and Table 4.

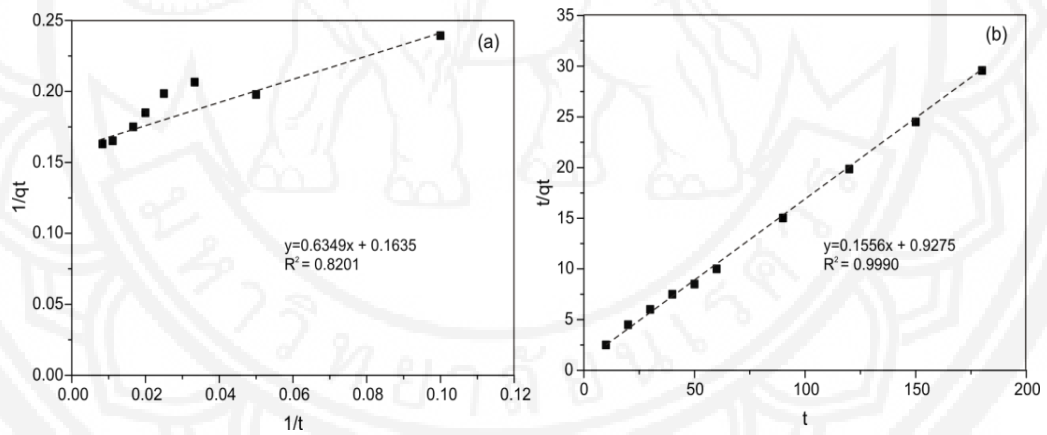


Figure 5 Kinetic plots for Cd(II) ions adsorption on pNGS; (a) pseudo first order and (b) pseudo second order.

Table 4 Kinetic parameters for Cd(II) ions adsorption

Kinetic parameters	Pseudo-first order				Pseudo-second order		
	q_{e1}	k_1	R^2	q_{e2}	k_2	R^2	
q_e (exp.)	6.11 mg g ⁻¹	3.88 min ⁻¹	0.8201	6.43 mg g ⁻¹	0.03 g mg ⁻¹ min ⁻¹	0.9990	

Based on the higher R^2 for the pseudo-second order model together with the experimental, the q_e values were close to the calculated q_{ca} , which supports the high applicability of this model to well-describe the experimental data.



It was implied that the adsorption process between Cd(II) ions and the active sites of the adsorbent had occurred through chemical sorption involving valance forces through the sharing or exchange of electrons between the heavy metal ions and the adsorbent (Feng, Guo, Liang, Zhu, & Liu, 2011; Mohammad, Saeid, & Hossein, 2016). In this type of adsorption, the molecules were not attracted by all the points on the surface of the solid, but were, instead, specifically attracted to the active sites. Initially, a single layer was formed, and other layers may have been formed by physisorption (Ho & McKay, 1999).

Isotherm study

Figure 6 shows Langmuir and Freundlich isotherms for Cd(II) ion adsorption. The adsorption parameters are summarized in Table 5. The results present that the R^2 of the Langmuir model was very close to 1 and was larger than the Freundlich model, which suggests that the adsorption was a process that had occurred on a homogeneous surface with monolayer adsorption. Moreover, the Langmuir model described the adsorption process and adsorption capacity of the metal ions based on the physical hypothesis (Afkhami, Madrakian, Karimi, & Amini, 2007).

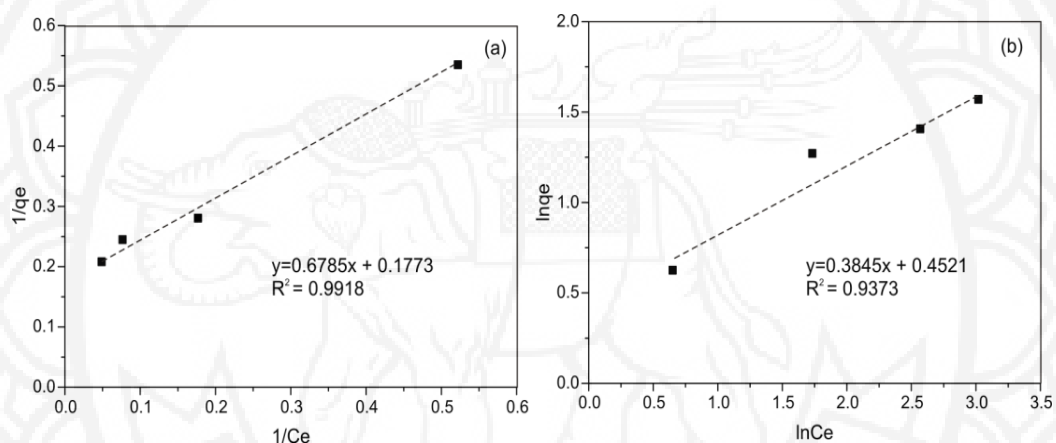


Figure 6 Langmuir and Freundlich isotherms for Cd(II) ions adsorption on pNGS

Table 5 Regression parameters for Langmuir and Freundlich adsorption isotherms for Cd(II) ions adsorption

Langmuir isotherm				Freundlich isotherm			
q_m (mg g^{-1})	K_L (L mg^{-1})	q_e (mg g^{-1})	R^2	K_F ($\text{mg g}^{-1})(\text{L mg}^{-1})^{1/n}$	$1/n$	q_e (mg g^{-1})	R^2
5.64	0.26	4.90	0.9918	1.57	0.39	7.07	0.9373

Thermodynamic study

The thermodynamic plot and parameters are presented in Figure 7 and Table 6. The obtained linear relation is $y = -1428.2x + 3.0484$ with an R^2 of 0.9798. Based on this equation, positive values of ΔH° were obtained, which suggests the endothermic nature of the adsorption process. The positive value of ΔS° had displayed a good affinity for Cd(II) ions towards the adsorbent and had increased the randomness at the solid-solution interface. The positive values of ΔG° indicated that the adsorbent system was non-spontaneous in nature. However, with an increase in the temperature from 298 K to 343 K, the ΔG° values were decreased. This revealed an increase in the adsorption of Cadmium and the trend towards spontaneous adsorption at higher temperatures (Denizli et al., 2000).

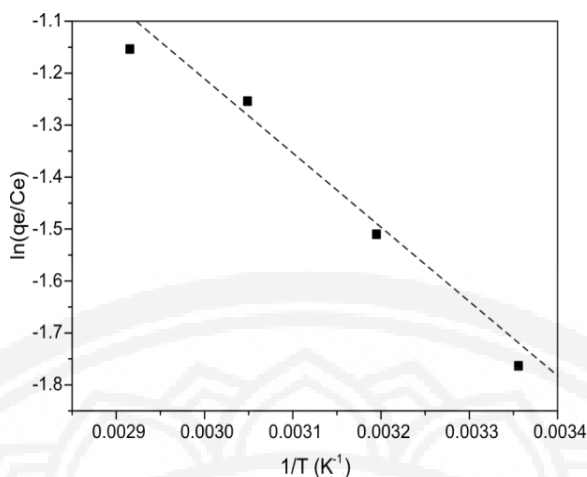


Figure 7 Thermodynamic plot for Cd(II) ions adsorption on pNGS

Table 6 Thermodynamic parameters for Cd(II) ions adsorption

ΔH° (KJ mol ⁻¹)	ΔS° (KJ mol ⁻¹)	ΔG° (KJ mol ⁻¹)			
		298 K	313 K	328 K	343 K
+ 11.874	+0.025	+ 4.335	+ 3.955	+ 3.576	+ 3.196

Comparison of the adsorption capacities and behaviors of various adsorbent for Cd(II) ions adsorption

The adsorption capacities of various bio-based adsorbents for removing Cd(II) ions are summarized in Table 7. It can be noted that the pNGS, derived in this work, had provided a relatively high adsorption capacity when compared to other bio-based adsorbents. Most of the adsorption isotherms are Langmuir, who described that the Cd(II) ions are adsorbed on the adsorbent surface via monolayer adsorption. The adsorption kinetics of the Cd (II) removal are all pseudo-second order, which implies that the adsorption had occurred through chemical sorption. Thermodynamic adsorption of most adsorbent is endothermic. Thus, the adsorption efficiency can be increased by increasing the temperature. Based on the literature, it can be concluded that pNGS can be employed as an alternative material for removing Cd(II) from aqueous solutions.

Table 7 Comparison of the adsorption capacities and behaviors of various adsorbents for Cd(II) ions adsorption

Adsorbents	Adsorption capacity (mg g ⁻¹)	Isotherm	Kinetic	Thermodynamic	Reference
Physic seed hull	11.89	Langmuir	*PSO	endothermic	Masita et al., 2010
Magnetic bio-char of pine bark waste	2.88	SIPS	*PSO		Reddy & Lee, 2013
Magnetic oak bark char	3.04	SIPS	*PSO		Mohan, Kumar, Sarswat, Alexandre-Franco, & Pittman, 2014
Magnetic acid-treated activated carbon	49.8	Langmuir	*PSO	endothermic	Abbass, Majid & Alireza, 2015

**Table 7** (Cont.)

Adsorbents	Adsorption capacity (mg g ⁻¹)	Isotherm	Kinetic	Thermodynamic	Reference
Modified Cassava peels(H ₂ SO ₄)	7.05	Langmuir	*PSO	endothermic	Daniel et al.,2016
Spent coffee grounds	4.48	Langmuir	*PSO	exothermic	María et al., 2017
Nature grape stem	1.78	Langmuir	*PSO	endothermic	Daniel, Affonso, Amarilis, & Alessandro, 2018
Turkish coffee grounds	1.32	Langmuir	*PSO	-	Aydeniz, Olcay, & Nazim, 2019
Iron-active biochar	2.97	Langmuir	*PSO	-	Liqiang et al., 2019
pNGS	5.90	Langmuir	*PSO	endothermic	This research

*PSO, pseudo-second order

Conclusion

Napier grass stems, which are an abundantly available agricultural residue in Thailand, can be utilized for removing Cd(II) ions from aqueous solutions, and these were examined based on process optimization. FT-IR and SEM results illustrated that metal ions could interact with active functional groups on the rough surface of the adsorbent. RSM was employed, while the influence of variables was evaluated from CCD and subsequently, the analysis of variance (ANOVA) was utilized. Based on a high F-value (43.29) and a p-value (<0.0001), the results indicated that the design had been statistically significant. Moreover, a high value of regression coefficient ($R^2=0.9750$) implied the validity of the model. The optimum conditions for adsorption were obtained with a solution pH of 5.83, an initial concentration of 50 mg L⁻¹, and an adsorbent dosage of 0.10 g. By using the optimum conditions, the obtained adsorption capacity was found to be 5.90 mg g⁻¹. The adsorption kinetic had corresponded to pseudo second-order kinetics, which rely on a process that may be chemical adsorption. The Langmuir isotherm model had best fitted the experimental results, as implied by the monolayer adsorption on the active surface site. Thermodynamic results indicated that the adsorption of Cd(II) on pNGS had been non-spontaneous and had been an endothermic process. Increases in adsorption were obtained at higher temperatures. Therefore, Napier grass stems can be considered to be a sustainable and alternative adsorbent for removing Cd(II) ions from aqueous solutions.

Acknowledgements

The author is thankful to Bureau of animal nutrition development, Khon Kaen, Thailand for their supporting the raw material. The author is grateful to Rajamangala University of Technology Isan (RMUTI), Khonkaen Campus, Khon Kaen, Thailand for providing fellowship for carrying out this research work. I am also kindly acknowledged the Department of Engineering, RMUTI for their foundation.



References

- Abbass, J. K., Majid, B., & Alireza, P. (2015). Removal of cadmium and lead from aqueous solutions by magnetic acid-treated activated carbon nanocomposite. *Desalination and Water Treatment*, 3994(40), 18782–18798.
- Afkhami, A., Madrakian, T., Karimi, Z., & Amini, A. (2007). Effect of treatment of carbon cloth with sodium hydroxide solution on its adsorption capacity for the adsorption of cations. *Colloids and Surfaces A: Physicochemical and Engineering Aspects*, 304(1–3), 36–40.
- Al-Malack, M. H., & Dauda, M. (2017). Competitive adsorption of cadmium and phenol on activated carbon produced from municipal sludge. *Journal of Environmental Chemical Engineering*, 5, 2718–2729.
- Al-Shannag, M., Al-Qodah, Z., Bani-Melhem, K., Qtaishat, M. R., & Alkasrawi, M. (2015). Heavy metal ions removal from metal plating wastewater using electrocoagulation: kinetic study and process performance. *Chemical Engineering Journal*, 260, 749–756.
- Aydeniz, D. D., Olcay, G., & Nazım, G. (2019). Optimization of adsorption for the removal of cadmium from aqueous solution using turkish coffee grounds. *International Journal of Environmental Research*, 13(5), 861–878.
- Bhargavi, M., Sethuraman, S., Krishnan, U. M., Bosco, J., & Rayappan, J. B. B. (2015). A review on detection of heavy metal ions in water – an electrochemical approach. *Sensors and Actuators B: Chemical*, 213, 515–533.
- Cai, X., He, J., Chen, L., Chen, K., Li, Y., Zhang, K., ... Wang, X. (2017). A₂D-g-C₃N₄ nanosheet as an eco-friendly adsorbent for various environmental pollutants in water. *Chemosphere*, 171, 192–201.
- Chabicovsky, M., Klepal, W., & Dallinger, R. (2004). Mechanism of cadmium toxicity in terrestrial pulmonates: programmed cell death and metallothionein overload. *Environmental Toxicology and Chemistry*, 23, 648–655.
- Daniel, S., Affonso, C. G. Jr., Gustavo, F. C., Marcelo, A. C., Douglas, C. D., César, R. T. T., ... Eduardo, A. V. L. (2016). Chemical modifications of cassava peel as adsorbent material for metals ions from wastewater. *Journal of Chemistry*, 2016(3694174), 15. <http://dx.doi.org/10.1155/2016/3694174>
- Daniel, S., Affonso, C. G. Jr, Amarilis, De V., & Alessandro, L. B. (2018). Modified grape stem as a renewable adsorbent for cadmium removal. *Water Science & Technology*, 78, 2308–2320.
- Denizli, A., Özkan, G., & Arica, Y. (2000). Preparation and characterization of magnetic polymethylmethacrylate microbeads carrying ethylene diamine for removal of Cu(II), Cd(II), Pb(II), and Hg(II) from aqueous solutions. *Journal of Applied Polymer*, 78(1), 81–89.
- Dil, E. A., Ghaedi, M., Mohammad, A., Asfaram, A., Mohammad, A., & Purkait, M. K. (2016). Application of artificial neural network and response surface methodology for the removal of crystal violet by zinc oxide nanorods loaded on activated carbon: kinetics and equilibrium study. *Journal of the Taiwan Institute of Chemical Engineers*, 59, 210–220.
- Feng, N., Guo, X., Liang, S., Zhu, Y., & Liu, J. (2011). Biosorption of heavy metals from aqueous solutions by chemically modified orange peel. *Journal of Hazardous Materials*, 185, 49–54.



- Freundlich, H. M. F. (1906). Over the adsorption in solution. *Journal of Physical Chemistry*, *57*, 385–471.
- Guo, X., Zhang, S., & Shan, X. Q. (2008). Adsorption of metal ions on lignin. *Journal of Hazardous Materials*, *151*, 134–142.
- Gupta, V. K., Tyagi, I., Sadegh, H., Shahryari-Ghoshekandi, R., Makhoulouf, A. S. H., & Maazinejad, B. (2015). Nanoparticles as adsorbent; a positive approach for removal of noxious metal ions: a review. *Science Technology and Development*, *34*(3), 195–214.
- Herbert, N., Affonso, C. G. Jr., Marcelo, A. C., Gustavo, F. C., Daniel, S., Marcelo, G. dos S., & Juliano, Z. (2016). Adsorption of Cu (II) and Zn (II) from Water by *Jatropha curcas* L. as Biosorbent. *Open Chemistry*, *14*, 103–117.
- Ho, Y. S., & McKay, G. (1999). Pseudo-second order model for sorption process. *Process Biochemistry*, *34*, 19451–19465.
- Karimi, M., Milani, S. A., & Abolghashemi, H. (2016). Kinetic and isotherm analyses for thorium (IV) adsorptive removal from aqueous solutions by modified magnetite nanoparticle using response surface methodology (RSM). *Journal of Nuclear Materials*, *479*, 174–183.
- Lagergren, S. (1898). About the theory of so-called adsorption of soluble substances. *Kungl. Svenska vetenskapsakademiens handlingar*, *24*, 1–39.
- Langmuir, I. (1918). The adsorption of gases on plane surfaces of glass, mica and platinum. *Journal of the American Chemical Society American Chemical Society*, *40*, 1361–1403.
- Leng, L., Yuana, X., Zenga, G., Shaoa, J., Chen, X., Wua, Z., ... & Peng, X. (2015). Surface characterization of rice husk bio-char produced by liquefaction and application for cationic dye (Malachite green) adsorption. *Fuel*, *155*, 77–85.
- Li, C., Zhao, S., Zhang, S., Shi, X., Zhu, D., & Sun, B. (2011). Analysis and evaluation of the source of heavy metals in water of the River Changjiang. *Environmental Monitoring and Assessment*, *173*, 301–313.
- Liqiang, C., Tianming, C., Chuntao, Y., Jinlong, Y., James, A. I., & Qaiser, H. (2019). Mechanism of adsorption of cadmium and lead ions by iron-activated biochar. *BioResources*, *14*(1), 842–857.
- Llanos, J., Williams, P. M., Cheng, S., Rogers, D., Wright, C., Pérez, A., & Cañizares, P. (2010). Characterization of a ceramic ultrafiltration membrane in different operational states after its use in a heavy-metal ion removal process. *Water Research*, *44*, 3522–3530.
- María, S. P., Irene, B., Jorge, E. S., & Franco, M. (2017). Cadmium removal from aqueous solution by adsorption on spent coffee grounds. *Chemical Engineering Transactions*, *60*, 157–162.
- Masita, M., Saikat, M., Naveed, A., Azmi, B., Sen, T. K., & Binay, K. D. (2010). Metal ion removal from aqueous solution using physic seed hull. *Journal of Hazardous Materials*, *179*, 363–372.
- Mohammad, K., Saeid, A. M., & Hossein, A. (2016). Kinetic and isotherm analyses for thorium (IV) adsorptive removal from aqueous solutions by modified magnetite nanoparticle using response surface methodology (RSM). *Journal of Nuclear Materials*, *479*, 174–183.



- Mohan, D., Kumar, H., Sarswat, A., Alexandre-Franco, M., & Pittman, C. U. (2014). Cadmium and lead remediation using magnetic oak wood and oak bark fast pyrolysis bio-chars. *Chemical Engineering Journal*, 236, 513–528.
- Montgomery, D. C., (2008). *Design and Analysis of Experiments*. New York: John Wiley & Sons.
- Pavan, F. A., Lima, E. C., Dias, S. L., & Mazzocato, A. C. (2008). Methylene blue biosorption from aqueous solutions by yellow passion fruit waste. *Journal of Hazardous Materials*, 150, 703–712.
- Peng, N., Hu, D., Zeng, J., Li, Y., Liang, L., & Chang, C. (2016). Superadsorbent cellulose–clay nanocomposite hydrogel for highly efficient removal of dye in water. *ACS Sustainable Chemistry & Engineering*, 4, 7217–7224.
- Qu, G., Liang, D., Qu, D., Huang, Y., Liu, T., Mao, H., ... Huang, D. (2013). Simultaneous removal of cadmium ions and phenol from water solution by pulsed corona discharge plasma combined with activated carbon. *Chemical Engineering Journal*, 228, 28–35.
- Reddy, D. H. K., & Lee, S-M. (2013). Application of magnetic chitosan composites for the removal of toxic metal and dyes from aqueous solutions. *Advances in Colloid and Interface Science*, 201–202, 68–93.
- Runping, H., Lijun, Z., Chen, S., Manman, Z., Huimin, Z., & LiJuan, Z. (2010). Characterization of modified wheat straw, kinetic and equilibrium study about copper ion and methylene blue adsorption in batch mode. *Carbohydrate Polymers*, 79(4), 1140–1149.
- Saad, M., Tahir, H., Khan, J., Hameed, U., & Saud, A. (2017). Synthesis of polyaniline nanoparticles and their application for the removal of Crystal Violet dye by ultrasonicated adsorption process based on response surface methodology. *Ultrasonics. Sonochemistry*, 34, 600–608.
- Sales, P. F., Magriotis, Z. M., Rossi, M. A. L. S., Resende, R. F., & Nunes, C. A. (2013). Optimization by response surface methodology of the adsorption of coomassie blue dye on natural and acid-treated clay. *Journal of Environmental Management*, 30, 417–428.
- Santra, D., & Sarkar, M. (2016). Optimization of process variables and mechanism of arsenic (V) adsorption onto cellulose nanocomposite. *Journal of Molecular Liquids*, 224, 290–302.
- Sun, T., Zhao, Z., Liang, Z., Liu, J., Shi, W., & Cui, F. (2017). Efficient removal of arsenite through photocatalytic oxidation and adsorption by $ZrO_2-Fe_3O_4$ magnetic nanoparticles. *Applied Surface Science*, 416, 656–665.
- Sun, Y., Zhou, Q., Xu, Y., Wang, L., & Liang, X. (2011). Phytoremediation for co-contaminated soils of benzo[a]pyrene (B[a]P) and heavy metals using ornamental plant *Tagetes patula*. *Journal of Hazardous Materials*, 186, 2075–2082.
- Tan, P., Sun, J., Hu, Y., Fang, Z., Bi, Q., Chen, Y., & Cheng, J. (2015). Adsorption of Cu^{2+} , Cd^{2+} and Ni^{2+} from aqueous single metal solutions on graphene oxide membranes. *Journal of Hazardous Materials*, 297, 251–260.
- Tatah, V. S., Ibrahim, K. L. C., Ezeonu, C. S., & Otitoju, O. (2017). Biosorption kinetics of heavy metals from Fertilizer industrial waste water using groundnut husk powder as an adsorbent. *Journal of Applied Biotechnology & Bioengineering*, 2(6), 221–228.



- Wang, Z., Feng, Y., Hao, X., Huang, W., & Feng, X. (2014). A novel potential-responsive ion exchange film system for heavy metal removal. *Journal of Materials Chemistry A*, *2*, 10263–10272.
- WHO. (2011). *Guidelines for Drinking-water Quality, fourth ed.*, World Health Organization, Geneva, Switzerland. Retrieved from https://www.who.int/water_sanitation_health/publications/2011/dwq_guidelines/en/
- Wimonrat, T., Orranooch, S., Titikan, S., & Manop, S. (2019). An alternative and cost-effective biosorbent derived from napier grass stem for malachite green removal. *Journal of Materials and Environmental Sciences*, *10*(8), 685–695.
- Wu, M., Liang, J., Jie, T., Li, G., Shan, S., Guo, Z., & Le, D. (2017). Decontamination of multiple heavy metals-containing effluents through microbial biotechnology. *Journal of Hazardous Materials*, *337*, 189–197.
- Xi, Y., Luo, Y., Luo, J., & Luo, X. (2015). Removal of cadmium (II) from waste water using novel cadmium ion-imprinted polymers. *Journal of Chemical & Engineering Data*, *60*(11), 3253–3261.
- Zhong, Y. J., You, S. J., Wang, X. H., Zhou, X., Gan, Y., & Ren, N. Q. (2013). Synthesis of carbonaceous nanowire membrane for removing heavy metal ions and high water flux. *Chemical Engineering Journal*, *226*, 217–226.
- Zhu, J., Baig, S. A., Sheng, T., Lou, Z., Wang, Z., & Xu, X. (2015). Fe_3O_4 and MnO_2 assembled on honeycomb briquette cinders (HBC) for arsenic removal from aqueous solutions. *Journal of Hazardous Materials*, *286*, 220–228.